Stem Cell Reports
Report
ISSCR
OPEN ACCESS

Prepubertal androgen signaling is required to establish male fat distribution

Zachary L. Sebo[1,2,5] and Matthew S. Rodeheffer[2,3,4,5,*]
[1]Department of Molecular, Cellular and Developmental Biology, Yale University, New Haven, CT, USA
[2]Department of Comparative Medicine, Yale University School of Medicine, 375 Congress Ave, New Haven, CT 06520, USA
[3]Department of Cellular and Molecular Physiology, Yale University, New Haven, CT, USA
[4]Yale Stem Cell Center, Yale University, New Haven, CT, USA
[5]Yale Program in Integrative Cell Signaling and Neurobiology of Metabolism, Yale University, New Haven, CT, USA
*Correspondence: matthew.rodeheffer@yale.edu
https://doi.org/10.1016/j.stemcr.2022.04.001

SUMMARY

Fat distribution is sexually dimorphic and is associated with metabolic disease risk. It is unknown if prepubertal sex-hormone signaling influences adult fat distribution. Here, we show that karyotypically male androgen-insensitive mice exhibit pronounced subcutaneous adiposity compared with wild-type males and females. This subcutaneous adipose bias emerges prior to puberty and is not due to differences in adipocyte size or rates of adipogenesis between visceral and subcutaneous fat. Instead, we find that androgen-insensitive mice lack an adequate progenitor pool for normal visceral-fat expansion during development, thus increasing the subcutaneous-to-visceral-fat ratio. Obesogenic visceral-fat expansion is likewise inhibited in these mice, yet their metabolic health is similar to wild-type animals with comparable total fat mass. Taken together, these data show that adult fat distribution can be determined prior to the onset of puberty by the relative number of progenitors that seed nascent adipose depots.

INTRODUCTION

Adipose tissue expands by increasing the size of existing adipocytes through lipid uptake (hypertrophy) and by the generation of new adipocytes from precursor cells (hyperplasia). The contribution of hyperplasia to fat-mass expansion depends on the total number of precursors capable of undergoing adipogenesis (Hedbacker et al., 2020) and the rate at which adipogenesis occurs (Wang et al., 2013; Jeffery et al., 2015, 2016). During development, hyperplasia and hypertrophy are engaged to rapidly establish adipose tissue (Häger et al., 1977; Han et al., 2011). Sex-specific fat distribution is thought to emerge during puberty in both mice and humans, with males preferentially accruing visceral fat and females subcutaneous fat. This occurs through differential rates of adipogenesis and sex hormone-dependent regulation of adipocyte hypertrophy in distinct adipose depots (Hirsch and Knittle, 1970; Knittle et al., 1979; Holtrup et al., 2017; Sebo and Rodeheffer, 2021). In mice, puberty typically initiates at the time of weaning, which is around post-natal day 21 (P21), and sexual maturity is reached between P35 and P42. Testosterone levels surge during gonad development in male embryos, as well as neonatally, then diminish until puberty (Clarkson and Herbison, 2016). Testosterone begins to rise at ~P25 in males and reaches adult levels by P50 (Barkley and Goldman, 1977). As previous studies have focused on characterizing fat distribution during or after puberty, it is not known if prepubertal adipose-tissue development impacts adult fat distribution.

In mice, subcutaneous adipocytes arise soon after birth, whereas visceral adipocytes do not become visible until 1 week of age (Birsoy et al., 2011; Han et al., 2011). The major visceral-fat pad in mice is physically attached to the gonads (uterus in females, epididymis in males), suggesting that the development of reproductive organs is coupled to the emergence of this depot and may impact sex-specific fat distribution. To test this, we sought to characterize how visceral and subcutaneous fat is established in male, female, and androgen-receptor-deficient XY (ARdY) mice. ARdY mice are karyotypically male, yet due to androgen insensitivity, they develop external genitalia of females. Internal reproductive structures are absent in these animals except for small, undescended testes. As a result, ARdY mice are infertile and represent an anatomic intermediate between males and females (Lyon and Hawkes, 1970). How fat distribution is affected in these animals is not known.

Here, we show that ARdY mice display a profound bias toward subcutaneous adiposity. This bias cannot be explained by differences in adipocyte size or different rates of adipogenesis in visceral and subcutaneous fat. Rather, we find that fat distribution in ARdY mice is distinguishable from wild-type males and females prior to puberty and is due to reduced progenitor seeding in nascent visceral fat. ARdY fat distribution is maintained in obesity, and ARdY metabolic health is similar to wild-type animals with comparable total fat mass. Taken together, these data show that the relative number of progenitor cells in nascent adipose depots can determine adult fat distribution in normal and obese conditions.

RESULTS

Subcutaneous adiposity dominates in ARdY mice

To characterize fat distribution in adult mice, we quantified the mass of visceral and subcutaneous adipose tissue at

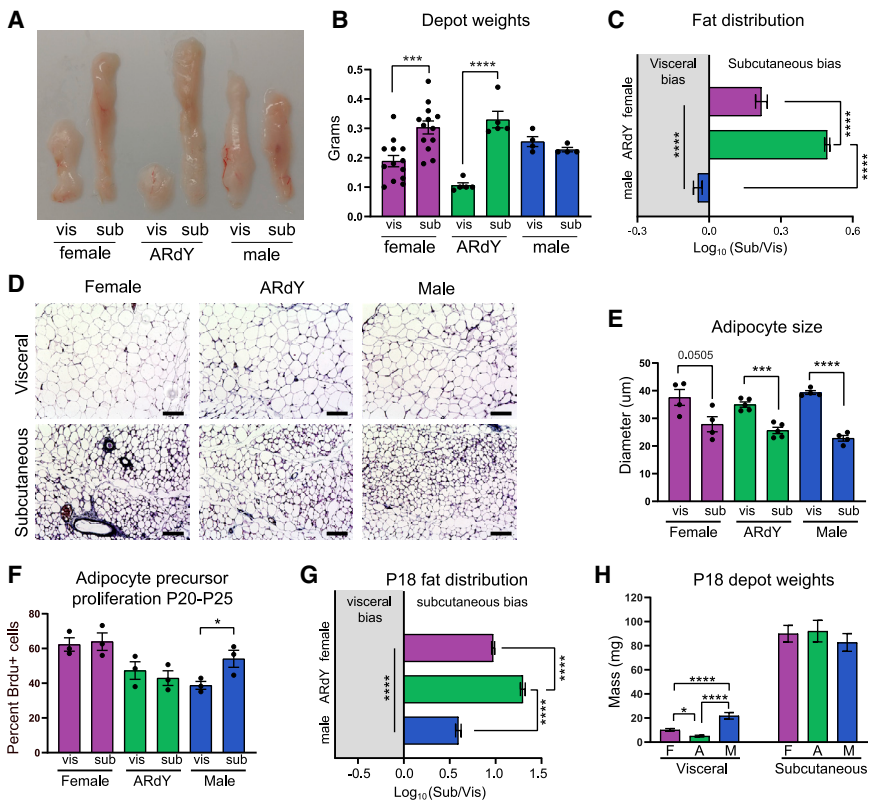

Figure 1. Subcutaneous adiposity dominates in ARdY mice

(A) Image of visceral and subcutaneous adipose depots of 7-week-old mice.

(B) Visceral and subcutaneous adipose depot weights of 7-week-old mice (n = 4–13).

(C) Fat distribution of 7-week-old mice (n = 4–13).

(D) Images of visceral and subcutaneous adipose tissue from 7-week-old mice.

(E) Adipocyte sizes from visceral and subcutaneous adipose depots of 7-week-old mice (n = 4–5).

(F) Adipocyte precursor proliferation of adolescent mice in visceral and subcutaneous adipose depots (n = 3).

(G) Fat distribution of 18-day-old mice (n = 11–23).

(H) Visceral and subcutaneous adipose depot weights of 18-day-old mice (n = 11–23).

Statistical significance in (B), (E), and (F) was determined by unpaired two-tailed Student's t test to compare depots within the same genotype. Statistical significance in (C), (G), and (H) was determined by ordinary one-way ANOVA with Tukey's multiple comparison's test. vis, visceral; sub, subcutaneous.

7 weeks of age. Consistent with previous literature, female mice have a greater proportion of subcutaneous fat compared with males (Figures 1A–1C and S1B). ARdY mice, on the other hand, exhibit even more pronounced subcutaneous adiposity, with approximately three times more subcutaneous fat than visceral fat (Figures 1A–1C). This size differential could be due to differences in the number of adipocytes or the respective sizes of those adipocytes (Jo et al., 2009). We found that subcutaneous adipocytes are smaller than visceral adipocytes in male, female, and ARdY mice (Figures 1D and 1E), indicating that the greater size of subcutaneous fat in female and ARdY mice is due to a higher number of adipocytes in this depot.

Total adipocyte number is determined by adipogenesis, and the rate of adipogenesis in visceral and subcutaneous fat during early puberty (P20–P25) is thought to contribute to sex-specific fat distribution in mice (Holtrup et al., 2017). However, we found no difference in adipocyte precursor proliferation (a prerequisite to adipogenesis; Figure 2I) between these depots from P20–P25 in ARdY mice (Figure 1F), suggesting that this developmental period does not impact fat distribution in these animals. Indeed, at P18, which is prior to the onset of puberty, ARdY mice already exhibit a subcutaneous-fat-mass bias significantly greater than males and females (Figure 1G). By directly comparing visceral- and subcutaneous-fat weights, we found that the visceral depot is smaller in ARdY mice compared with males and females at this age, with no differences in subcutaneous-fat weights or body weights (Figures 1H, S1C, and S1D). The amount of female visceral fat is also smaller than males at this age (Figures 1H and S1D). Importantly, ARdY visceral adipose mass as a percentage of body weight is significantly reduced compared with males and females at P18 and 7 weeks of age (Figures S1B and S1D). Together, these data indicate that prepubertal growth of visceral adipose tissue is impaired in ARdY mice.

ARdY fat distribution is determined by reduced progenitor seeding in nascent visceral fat

Given these prepubertal differences in visceral-fat mass, it is possible that developmental adipogenesis occurs at different rates in the visceral fat of male, female, and ARdY mice. Therefore, we quantified adipocyte formation from embryonic day 18.5 (E18.5) to P18 (Figure 2K) and P4 to P18 (Figure 2L) to identify if adipogenesis is altered among sexes at these developmental time points. As adipogenesis requires the proliferation of adipocyte precursor cells, we treated animals at E18.5 or P4 with BrdU (a thymidine analog that is incorporated into the DNA of

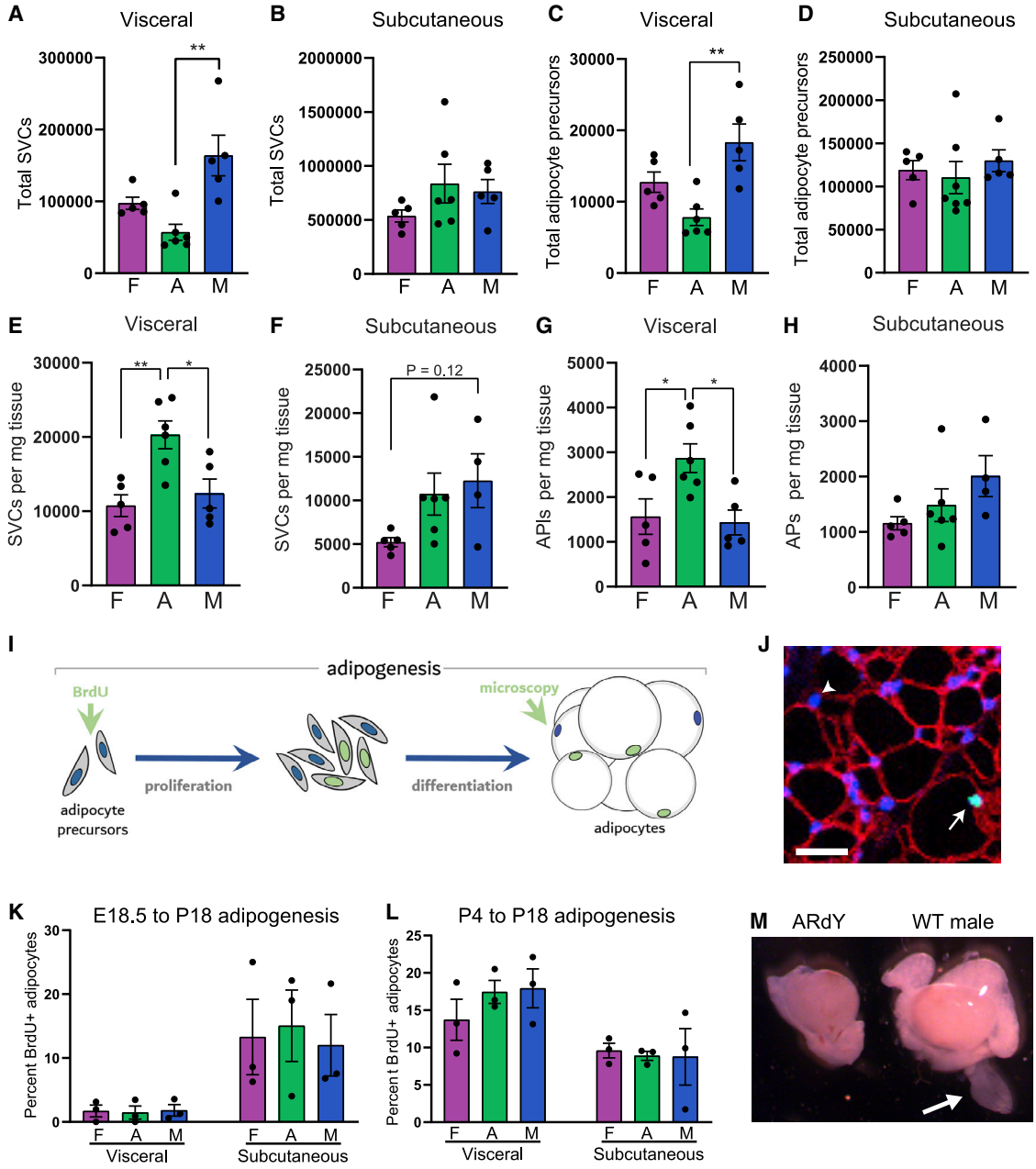

Figure 2. ARdY fat distribution is determined by reduced progenitor seeding in nascent visceral fat

(A) Total stromal vascular cells (SVCs) in visceral fat of 18- to 21-day-old mice (n = 5–6).

(B) Total SVCs in subcutaneous fat of 18- to 21-day-old mice (n = 5–6).

(C) Total adipocyte precursor cells in visceral fat of 18- to 21-day-old mice (n = 4–6).

(D) Total adipocyte precursor cells in subcutaneous fat of 18- to 21-day-old mice (n = 4–6).

(E) SVCs per mg visceral fat (n = 5–6).

(F) SVCs per mg subcutaneous fat (n = 4–6).

(G) Adipocyte precursors per mg visceral fat (n = 5–6).

(H) Adipocyte precursors per mg subcutaneous fat (n = 4–6).

(I) Schematic of adipogenesis *in vivo*.

(J) Image showing how BrdU+ adipocytes are identified. Arrowhead shows DAPI+ adipocyte nucleus. Arrow shows BrdU+/DAPI+ adipocyte nucleus. Non-adipocyte nuclei are surrounded by stained plasma membranes, as described in Jeffery et al. (2015). Scalebar, 25 μm.

(K) New adipocyte formation from E18.5 to P18 (n = 3).

(legend continued on next page)

proliferating cells) and quantified BrdU+ adipocyte nuclei at P18 by immunohistochemistry (as described in Jeffery et al., 2015) to assess adipogenesis (Figures 2I and 2J). Surprisingly, no differences in the amount of adipocyte formation were observed between males, females, and ARdY mice in either visceral- or subcutaneous-fat depots (Figures 2K and 2L), indicating that differential adipogenesis rates between depots do not contribute to prepubertal differences in fat distribution in ARdY mice.

Another factor that can impact fat mass is the total number of adipocyte precursors available to differentiate, as reducing the number of differentiation-competent progenitors lowers fat mass in adulthood and limits fat expansion in obesity (Hedbacker et al., 2020). Importantly, progenitor-pool size is independent of progenitor density. The term progenitor pool refers to the total number of adipocyte precursor cells within a given adipose depot. Progenitor density refers to the number of adipocyte precursor cells per unit tissue mass. Thus, it is possible that ARdY mice have a reduced visceral adipocyte precursor pool such that, even with a normal rate of adipogenesis, fewer adipocytes ultimately form. Consistent with this hypothesis, juvenile ARdY mice between 18 and 21 days of age have fewer visceral adipocyte precursors (Figure 2C) and total stromal vascular cells (SVCs) (Figure 2A) than males of the same age. A similar trend is observed compared with females (Figures 2A and 2C). In contrast, there are no differences in SVC or adipocyte precursor numbers among sexes for subcutaneous fat (Figures 2B and 2D). We next assessed adipocyte precursor density in juvenile mice and found that ARdY visceral fat has elevated precursor density compared with males and females (Figure 2G), indicating that the total number of adipocyte precursors—not the number of precursors per unit tissue mass—limits ARdY visceral-fat expansion. To further explore the possibility that nascent visceral fat in ARdY mice possess a reduced progenitor pool compared with males, we examined these animals for the presence of epididymal appendages at 4 days of age. Epididymal appendages are transient developmental structures composed predominately of adipocyte progenitors from which epididymal visceral fat forms in male mice (Han et al., 2011). Strikingly, epididymal appendages are absent in ARdY mice (Figure 2M). Taken together, these data support the conclusion that the reduced visceral-fat mass in ARdY mice is due to a dramatic reduction in visceral progenitor cell seeding during development.

Obesogenic visceral fat expansion is restricted in ARdY mice

Given that visceral fat expansion is impeded during development in ARdY mice, we hypothesized that obesogenic visceral fat expansion would also be limited in these animals. To test this, we fed male, female, and ARdY mice a high-fat diet (HFD) for a period of 8 weeks starting at 7 weeks of age, along with age-matched controls on a standard diet (SD). At 15 weeks of age, under both dietary conditions, ARdY body weight is between that of males and females, and ARdY lean mass is similar to females (Figures 3A and 3B). Notably, ARdY mice accumulate more total fat mass on SD than wild-type animals (Figures 3C and 3D), consistent with previous findings that show an age-associated increase in fat mass in androgen-insensitive mice (Sato et al., 2003). However, after 8 weeks of HFD, ARdY mice gain a similar amount of fat as males (Figure 3C). As expected, ARdY mice exhibit reduced visceral fat growth on an HFD, resulting in subcutaneous obesity (Figures 3E and 3F). It has previously been shown that obesogenic visceral adipogenesis is normal in ARdY mice (Sebo and Rodeheffer, 2021), indicating the reduced visceral fat growth in these animals is not due to impaired adipocyte differentiation. Moreover, adipocyte hypertrophy and the rate of adipocyte death, as measured by the prevalence of crown-like structures, are unaffected in ARdY mice compared with males (Figures 4A–4C). Therefore, these data indicate that obesogenic visceral fat growth in ARdY mice is limited by having a smaller initial cell number at the onset of expansion.

Since subcutaneous obesity is associated with better metabolic health than visceral obesity, we sought to explore the metabolic health of ARdY mice compared with males and females. To do this, we first performed glucose tolerance tests (GTTs), which are used to assess the dynamic response to a glucose challenge. Impaired glucose handling is marked by elevated blood glucose levels. Under SD conditions, ARdY mice exhibit impaired glucose handling compared with male and female mice (Figures S2A, S2C, and S2D), consistent with the increased fat mass in ARdY mice on SD (Figure 3C). However, under HFD conditions, ARdY mice display modestly improved glucose parameters compared with males, which have similar total fat mass, but not females, which have less total fat mass (Figures 3C and S2B–S2D). As ectopic lipid deposition is associated with insulin resistance (Samuel and Shulman, 2012) and may be reduced in subcutaneous obesity (Ibrahim, 2010), we quantified the lipid content of

(L) New adipocyte formation from P4 to P18 (n = 3).

(M) Image of P4 testis and surrounding structures in ARdY and male mice. Arrow shows epididymal appendage. Statistical significance was determined by ordinary one-way ANOVA with Tukey's multiple comparison's test. AP, adipocyte precursor; F, female; A, ARdY; M, male; WT, wild type.

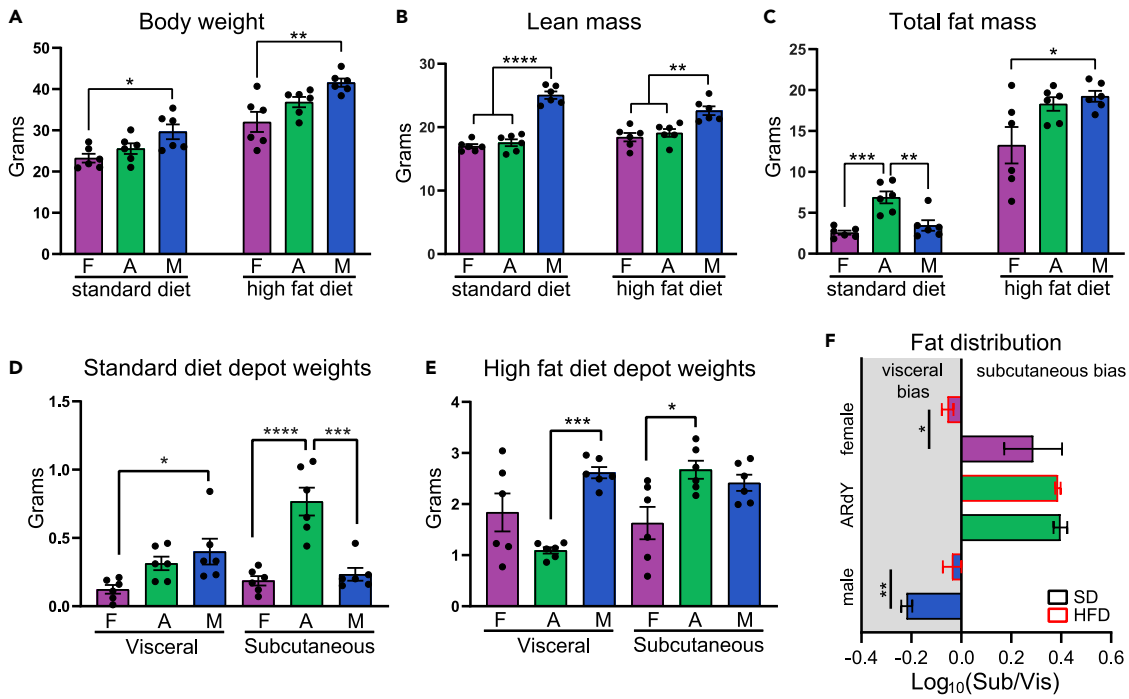

Figure 3. ARdY mice develop subcutaneous obesity on a high-fat diet (HFD) due to reduced visceral-fat growth

(A) Body weight of 15-week-old mice fed either a standard diet or an HFD (n = 6).

(B) Lean mass of 15-week-old mice fed either a standard diet or an HFD as determined by MRI (n = 6).

(C) Total fat mass of 15-week-old mice fed either a standard diet or an HFD as determined by MRI (n = 6).

(D) Visceral and subcutaneous depot weights of 15-week-old mice on standard diet (n = 6).

(E) Visceral and subcutaneous depot weights of 15-week-old mice on HFD (n = 6).

(F) Fat distribution of 15-week-old mice on standard diet or HFD (n = 6).

Statistical significance in (A)–(E) was determined by ordinary one-way ANOVA with Tukey's multiple comparisons test. Statistical significance in (F) was determined by an unpaired two-tailed Student's t test. F, female; A, ARdY; M, male; Sub, subcutaneous; Vis, visceral.

liver, gastrocnemius muscle, and heart. Interestingly, we found no appreciable differences in ectopic lipid deposition in these tissues among animals with similar total fat mass (Figures S3A–S3D). Indeed, a specific role for fat distribution in the metabolic phenotypes of ARdY mice is difficult to ascertain, as sex-specific differences unrelated to fat distribution are known to influence metabolic disease severity (Mauvais-Jarvis, 2015; Tramunt et al., 2020). For example, adiponectin activity, which is inhibited by androgen signaling, improves glucose metabolism and is present at higher levels in female and ARdY mice compared with males (Figure S2E) (Nishizawa et al., 2002; Pajvani and Scherer, 2003). Liver lipid metabolism also displays sexual dimorphism and could explain the sex-specific lipid accumulation in this organ (Figures S3A and S3B) (Zhang et al., 2011). Taken together, these data show that ARdY mice are predisposed to subcutaneous obesity by reduced visceral adipocyte progenitor seeding and that ARdY metabolic health is likely influenced by multiple factors that differentially overlap with males and females.

DISCUSSION

In this study, we sought to characterize the cellular mechanism by which fat distribution is established in ARdY mice compared with males and females. We found that ARdY mice exhibit dramatically reduced visceral fat mass under normal and obese conditions. This phenotype cannot be attributed to defects in adipogenesis or adipocyte hypertrophy nor to enhanced adipocyte death. Rather, ARdY mice lack epididymal appendages, perinatal structures that harbor progenitor cells of visceral fat (Han et al., 2011). Combined with previous work demonstrating that developmental progenitor seeding is an important determinant of adult fat mass (Hedbacker et al., 2020), our data show that a lower number of progenitor cells in nascent visceral fat are responsible for limiting the subsequent growth of this depot in ARdY mice. Thus, prepubertal androgen signaling is necessary for the establishment of normal visceral adipose mass in male mice. Our data also suggest that visceral progenitor seeding is modestly less in females compared with males. This difference in progenitor

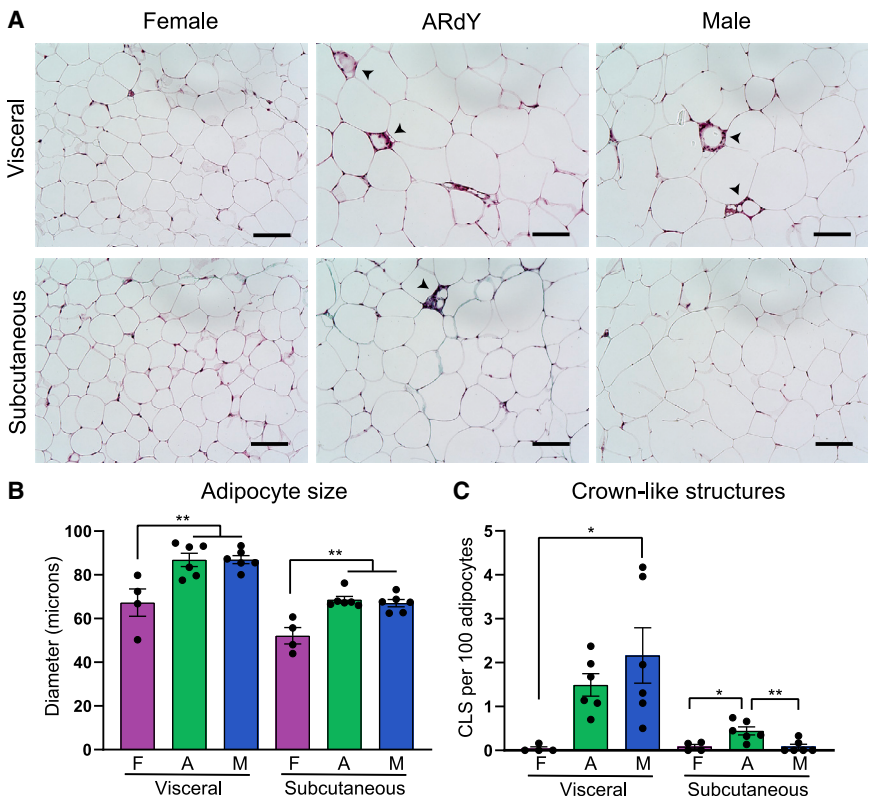

Figure 4. Adipocyte hypertrophy and adipocyte death are normal in obese ARdY visceral fat

(A) Representative images of visceral and subcutaneous fat in 15-week-old mice fed HFD for 8 weeks. Arrowheads show crown-like structures. Scalebar, 100 μm.

(B) Adipocyte size in visceral and subcutaneous fat of 15-week-old mice fed HFD for 8 weeks (n = 4–6).

(C) Crown-like structures per 100 adipocytes in visceral and subcutaneous fat of 15-week-old mice fed HFD for 8 weeks (n = 4–6).

Statistical significance in (B) and (C) was determined by ordinary one-way ANOVA with Tukey's multiple comparisons test. F, female; A, ARdY; M, male.

seeding could explain the prepubertal differences in fat distribution between the sexes. However, given that females lack a comparable structure to the epididymal appendage of males, this is difficult to confirm.

In the future, it will be important to characterize the embryonic-patterning mechanisms responsible for depot-specific progenitor seeding. Indeed, it has been shown that visceral fat is derived from distinct mesodermal subcompartments in male and female mice. In males, approximately 60% of visceral adipocytes are derived from the somites, with the remaining 40% of unknown origin (Sebo et al., 2018). Given that androgen signaling is required for the development of the epididymis from the intermediate mesoderm (IM) (Drago, 2014; Murashima et al., 2015a, 2015b), it is possible that the remaining 40% of adipocytes are derived from IM, and ARdY visceral fat lacks cells from this lineage. Equally plausible is that progenitor migration from the somitic mesoderm to the presumptive epididymal appendage is disrupted. The origin of female visceral fat, on the other hand, is entirely lateral plate mesoderm (Sebo et al., 2018). How the female visceral progenitor field is established in concert with reproductive organs remains an open question.

It is noteworthy that fat distribution in ARdY mice was not clearly associated with metabolic phenotypes. Through considerable effort in the last two decades, it has become clear that the relationship between fat distribution and metabolic disease is multifactorial, involving numerous hormones, diet, and age (Cnop et al., 2003; Paniagua et al., 2007; Sebo and Rodeheffer, 2021). Our data support this notion and show that the level of depot-specific progenitor seeding during development can determine adult fat distribution and the ability of fat depots to expand in obesity. Parsing whether such a mechanism contributes to metabolic disease will require the development of novel mouse models that permit the selective ablation of a subset of adipocyte progenitors in specific nascent adipose depots without altering the hormonal environment.

EXPERIMENTAL PROCEDURES

Animals and assessment of fat distribution

Animal experiments were performed according to Yale University's Institutional Animal Care and Use Committee (IACUC). ARdY mice (Lyon and Hawkes, 1970) were obtained from Jackson Laboratories (Stock #001809) and maintained on the C57BL/6J-A$^{w\text{-}j}$/J background. The Eda$^{Ta\text{-}6J}$ marker mutation was bred out of the strain prior to experiments. Littermates were used in all experiments. The SD in this study was made by Harlan Laboratories (2018S) and the HFD by Research Diets (D12492). The body composition of mice was determined via magnetic resonance imaging (EchoMRI-100H, EchoMRI, Houston, TX, USA).

Fat distribution was calculated using the following equation:

$$log\ 10\left(\frac{SWAT}{VWAT}\right),$$

where the weight in grams of subcutaneous (inguinal) and visceral (perigonadal) depots were divided to acquire a subcutaneous white adipose tissue (SWAT)/visceral white adipose tissue (VWAT) ratio. The logarithm of this ratio is required to correct for skew.

Flow-cytometry analysis of SVCs and adipocyte precursors

To determine the number of SVCs and adipocyte precursors in whole-adipose depots, adipose tissue was minced and digested in Hank's balanced salt solution (HBSS) (Sigma; H8264) containing 3% BSA and 0.8 mg mL^{-1} Collagenase Type 2 (Worthington Biochemical; LS004174) for approximately 75 min in a 37°C shaking water bath. The digest solution was then filtered through a 40-um filter, pelleted by a brief centrifugation (300 × *g* for 3 min), and washed in HBSS +3% BSA. Cell pellets (which contain all SVCs) were stained with a previously described antibody cocktail (Berry and Rodeheffer, 2013) and analyzed by flow cytometry (BD LSRII). All stained cells contributed to the SVC count, whereas adipocyte precursors were distinguished by their unique cell-surface-marker profile (Berry and Rodeheffer, 2013; Jeffery et al., 2015, 2016). To quantify adipocyte precursor proliferation from P20 to P25, mice were given BrdU in their drinking water (0.8 mg/mL) during this period of time, and adipose tissue was digested as above. Cell pellets were stained with a previously described antibody cocktail and further processed for BrdU quantification by flow cytometry (Jeffery et al., 2015).

Adipocyte hyperplasia, hypertrophy, and crown-like-structures

To quantify adipocyte formation from E18.5 to P18, pregnant dams were injected intraperitoneally with 50 mg/kg BrdU in PBS. Adipocyte nuclei from pups of such litters were analyzed for BrdU incorporation at P18. Similarly, to quantify adipocyte formation from P4 to P18, P4 pups were injected intraperitoneally with 50 mg/kg BrdU in PBS in the morning and evening and allowed to develop until P18, at which point BrdU incorporation into adipocyte nuclei was quantified. At least 100 BrdU+ adipocytes were counted for each depot. Adipocyte size and crown-like structures were determined from images of trichrome-stained histological sections of adipose tissue using Cell Profiler and ImageJ (Abràmoff et al., 2004; Carpenter et al., 2006). At least 50 adipocytes per depot of each animal were quantified for sizing, and a total of at least 500 adipocytes per depot of each animal were counted for crown-like-structures. Histological sectioning and trichrome staining were performed by the Histology Core Laboratory of the Yale School of Medicine, Department of Comparative Medicine. Images were taken using a Leica SP5 confocal microscope for the quantification of BrdU+ adipocyte nuclei and a Keyence BZ-X800 microscope for adipocyte sizing and crown-like-structure quantification.

Metabolic assessments

For GTTs, mice were fasted overnight (16–18 h), and fasting blood glucose level was obtained via a tail-vein nick. Mice were injected intraperitoneally with a 20% glucose solution in saline at 2 g/glucose/kg body weight, and blood glucose was measured at 10, 20, 30, 60, and 120 min afterward. Glucose tolerance is defined as the incremental area under the curve (i.e., the area under the curve normalized to fasting glucose). Adiponectin ELISA (Crystal Chem, catalog #80569) was performed according to manufacturer's instructions. Tissue lipid quantification in liver, gastrocnemius, and heart was performed using the Cell Biolabs Fluorometric Lipid Quantification Kit (catalog #STA-617) according to manufacturer's instructions, with reagent volumes halved in technical singlicate. For oil red O staining, the medial lobe of the liver was fixed in 4% paraformaldehyde for ∼24 h followed by incubation in 30% sucrose in saline for ∼24 h. Livers were then embedded in optimal cutting temperature (OCT) compound (Tissue-Tek, product code 4583) and flash frozen in liquid nitrogen. Histological sectioning and oil red O staining was performed by the Histology Core Laboratory of the Yale School of Medicine, Department of Comparative Medicine. Bright-field images of histological sections were taken using a Keyence BZ-X800 microscope.

Statistical analysis

Statistical tests were performed using GraphPad Prism (v.8.3.0). p values <0.05 were considered significant. The specific statistical tests used for each experiment and the number of biological replicates are denoted in the figure legends. Error bars represent mean ± SEM. *p < 0.05, **p < 0.01, ***p < 0.001, ****p < 0.0001.

SUPPLEMENTAL INFORMATION

Supplemental information can be found online at https://doi.org/10.1016/j.stemcr.2022.04.001.

AUTHOR CONTRIBUTIONS

Z.L.S. conceived of the project, performed experiments, analyzed data, and wrote the paper. M.S.R. analyzed data, supervised the project, and edited the paper.

CONFLICTS OF INTEREST

The authors declare no competing interests.

ACKNOWLEDGMENTS

The authors thank Michael Schadt and the Histology Core Laboratory for assistance with tissue sectioning and staining. We also thank Caroline Zeiss for sharing microscopy equipment and the Yale Flow Cytometry Core for equipment usage. This work was supported by a National Science Foundation Graduate Research Fellowship (DGE1122492 to Z.L.S.) and the NIDDK (R01DK110147 and DK090489 to M.S.R.).

Received: June 22, 2021
Revised: March 30, 2022
Accepted: April 1, 2022
Published: April 28, 2022

REFERENCES

Abràmoff, M.D., Magalhães, P.J., and Ram, S.J. (2004). Image processing with ImageJ. Biophotonics Int. *11*, 36–42.

Barkley, M.S., and Goldman, B.D. (1977). A quantitative study of serum testosterone, sex accessory organ growth, and the development of intermale aggression in the mouse. Horm. Behav. *8*, 208–218.

Berry, R., and Rodeheffer, M.S. (2013). Characterization of the adipocyte cellular lineage in vivo. Nat. Cell Biol. *15*, 302–308.

Birsoy, K., Berry, R., Wang, T., Ceyhan, O., Tavazoie, S., Friedman, J.M., and Rodeheffer, M.S. (2011). Analysis of gene networks in white adipose tissue development reveals a role for ETS2 in adipogenesis. Development *138*, 4709–4719.

Carpenter, A.E., Jones, T.R., Lamprecht, M.R., Clarke, C., Kang, I.H., Friman, O., Guertin, D.A., Chang, J.H., Lindquist, R.A., and Moffat, J. (2006). CellProfiler: image analysis software for identifying and quantifying cell phenotypes. Genome Biol. *7*, R100.

Clarkson, J., and Herbison, A.E. (2016). Hypothalamic control of the male neonatal testosterone surge. Philos. Trans. R. Soc. B Biol. Sci. *371*, 20150115.

Cnop, M., Havel, P.J., Utzschneider, K., Carr, D., Sinha, M., Boyko, E., Retzlaff, B., Knopp, R., Brunzell, J., and Kahn, S.E. (2003). Relationship of adiponectin to body fat distribution, insulin sensitivity and plasma lipoproteins: evidence for independent roles of age and sex. Diabetologia *46*, 459–469.

Drago, M. (2014). Androgen Insensitivity Syndrome (Embryo Project Encyclopedia).

Häger, A., Sjöström, L., Arvidsson, B., Björntorp, P., and Smith, U. (1977). Body fat and adipose tissue cellularity in infants: a longitudinal study. Metabolism *26*, 607–614.

Han, J., Lee, J.-E., Jin, J., Lim, J.S., Oh, N., Kim, K., Chang, S.-I., Shibuya, M., Kim, H., and Koh, G.Y. (2011). The spatiotemporal development of adipose tissue. Development *138*, 5027–5037.

Hedbacker, K., Lu, Y.-H., Dallner, O., Li, Z., Fayzikhodjaeva, G., Birsoy, K., Han, C., Yang, C., and Friedman, J.M. (2020). Limitation of adipose tissue by the number of embryonic progenitor cells. Elife *9*, e53074.

Hirsch, J., and Knittle, J.L. (1970). Cellularity of obese and nonobese human adipose tissue. Fed. Proc. *29*, 1516–1521.

Holtrup, B., Church, C.D., Berry, R., Colman, L., Jeffery, E., Bober, J., and Rodeheffer, M.S. (2017). Puberty is an important developmental period for the establishment of adipose tissue mass and metabolic homeostasis. Adipocyte *6*, 224–233.

Ibrahim, M.M. (2010). Subcutaneous and visceral adipose tissue: structural and functional differences. Obes. Rev. *11*, 11–18.

Jeffery, E., Church, C.D., Holtrup, B., Colman, L., and Rodeheffer, M.S. (2015). Rapid depot-specific activation of adipocyte precursor cells at the onset of obesity. Nat. Cell Biol. *17*, 376–385.

Jeffery, E., Wing, A., Holtrup, B., Sebo, Z., Kaplan, J.L., Saavedra-Peña, R., Church, C.D., Colman, L., Berry, R., and Rodeheffer, M.S. (2016). The adipose tissue microenvironment regulates depot-specific adipogenesis in obesity. Cell Metabol. *24*, 142–150.

Jo, J., Gavrilova, O., Pack, S., Jou, W., Mullen, S., Sumner, A.E., Cushman, S.W., and Periwal, V. (2009). Hypertrophy and/or hyperplasia: dynamics of adipose tissue growth. PLoS Comput. Biol. *5*, e1000324.

Knittle, J., Timmers, K., Ginsberg-Fellner, F., Brown, R., and Katz, D. (1979). The growth of adipose tissue in children and adolescents. Cross-sectional and longitudinal studies of adipose cell number and size. J. Clin. Invest. *63*, 239–246.

Lyon, M.F., and Hawkes, S.G. (1970). X-linked gene for testicular feminization in the mouse. Nature *227*, 1217–1219.

Mauvais-Jarvis, F. (2015). Sex differences in metabolic homeostasis, diabetes, and obesity. Biol. Sex Differ. *6*, 1–9.

Murashima, A., Kishigami, S., Thomson, A., and Yamada, G. (2015a). Androgens and mammalian male reproductive tract development. Biochim. Biophys. Acta *1849*, 163–170.

Murashima, A., Xu, B., and Hinton, B.T. (2015b). Understanding normal and abnormal development of the Wolffian/epididymal duct by using transgenic mice. Asian J. Androl. *17*, 749.

Nishizawa, H., Shimomura, I., Kishida, K., Maeda, N., Kuriyama, H., Nagaretani, H., Matsuda, M., Kondo, H., Furuyama, N., and Kihara, S. (2002). Androgens decrease plasma adiponectin, an insulin-sensitizing adipocyte-derived protein. Diabetes *51*, 2734–2741.

Pajvani, U.B., and Scherer, P.E. (2003). Adiponectin: systemic contributor to insulin sensitivity. Curr. Diabetes Rep. *3*, 207–213.

Paniagua, J.A., De La Sacristana, A.G., Romero, I., Vidal-Puig, A., Latre, J., Sanchez, E., Perez-Martinez, P., Lopez-Miranda, J., and Perez-Jimenez, F. (2007). Monounsaturated fat–rich diet prevents central body fat distribution and decreases postprandial adiponectin expression induced by a carbohydrate-rich diet in insulin-resistant subjects. Diabetes Care *30*, 1717–1723.

Samuel, V.T., and Shulman, G.I. (2012). Mechanisms for insulin resistance: common threads and missing links. Cell *148*, 852–871.

Sato, T., Matsumoto, T., Yamada, T., Watanabe, T., Kawano, H., and Kato, S. (2003). Late onset of obesity in male androgen receptor-deficient (AR KO) mice. Biochem. Biophys. Res. Commun. *300*, 167–171.

Sebo, Z.L., and Rodeheffer, M.S. (2021). Testosterone metabolites differentially regulate obesogenesis and fat distribution. Mol. Metabol. *44*, 101141.

Sebo, Z.L., Jeffery, E., Holtrup, B., and Rodeheffer, M.S. (2018). A mesodermal fate map for adipose tissue. Development *145*, dev166801.

Tramunt, B., Smati, S., Grandgeorge, N., Lenfant, F., Arnal, J.-F., Montagner, A., and Gourdy, P. (2020). Sex differences in metabolic regulation and diabetes susceptibility. Diabetologia *63*, 453–461.

Wang, Q.A., Tao, C., Gupta, R.K., and Scherer, P.E. (2013). Tracking adipogenesis during white adipose tissue development, expansion and regeneration. Nat. Med. *19*, 1338–1344.

Zhang, Y., Klein, K., Sugathan, A., Nassery, N., Dombkowski, A., Zanger, U.M., and Waxman, D.J. (2011). Transcriptional profiling of human liver identifies sex-biased genes associated with polygenic dyslipidemia and coronary artery disease. PLoS One *6*, e23506.

Stem Cell Reports, Volume *17*

Supplemental Information

Prepubertal androgen signaling is required to establish male fat distribution

Zachary L. Sebo and Matthew S. Rodeheffer

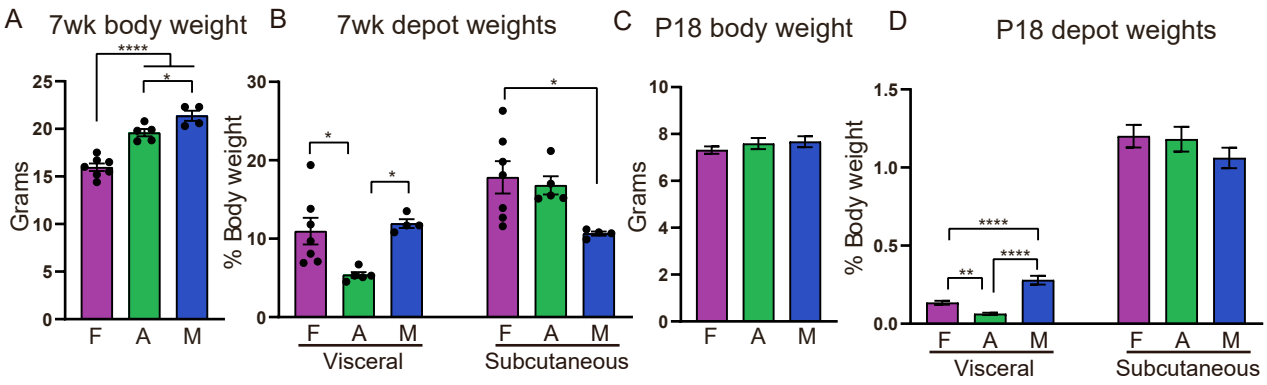

Supp. Fig. 1. Young adult and juvenile fat distribution, related to Figure 1. (A) Body weight of 7-week-old mice (n = 4-7). (B) Depot weights as a percentage of body weight for 7-week-old mice (n = 4-7). (C) Body weight of P18 mice (n = 11-23). (D) P18 depot weights as a percentage of body weight (n = 11-23). Statistical significance was determined by ordinary one-way ANOVA with Tukey's multiple comparisons test. Abbreviations: F = female, A = ARdY, M = male, SVC = stromal vascular cell, AP = adipocyte precursor.

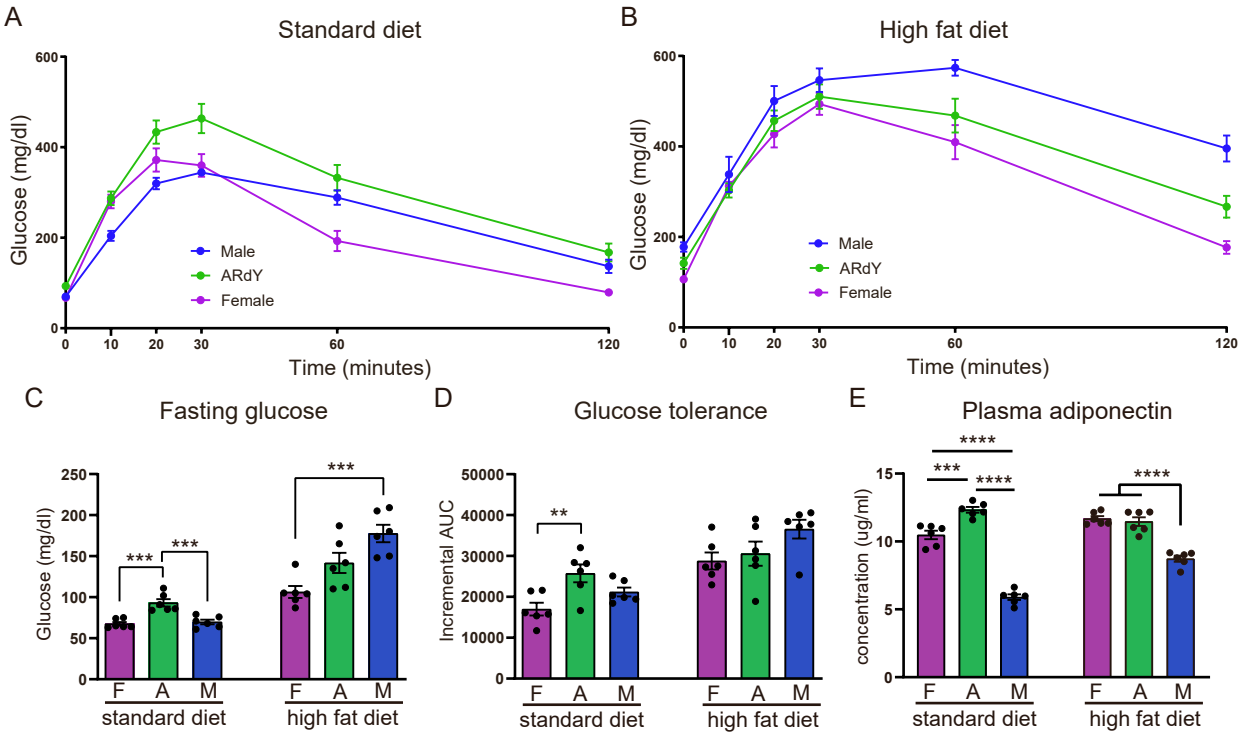

Supp. Fig. 2. Glucometabolic health parameters in SD and HFD, related to Figure 3. (A) GTT curve of 15-week-old mice fed standard diet (n = 6). (B) GTT curve of 15-week-old mice fed high fat diet (n = 6). (C) Fasting glucose of 15-week-old mice from (A) and (B) (n = 6). (D) Glucose tolerance as measured by iAUC from animals in (A-C). (E) Plasma adiponectin level in mice from (A-D) (n = 6). Statistical significance in (C-E) was determined by ordinary one-way ANOVA with Tukey's multiple comparisons test. Abbreviations: F = female, A = ARdY, M = male, iAUC = incremental area under the curve.

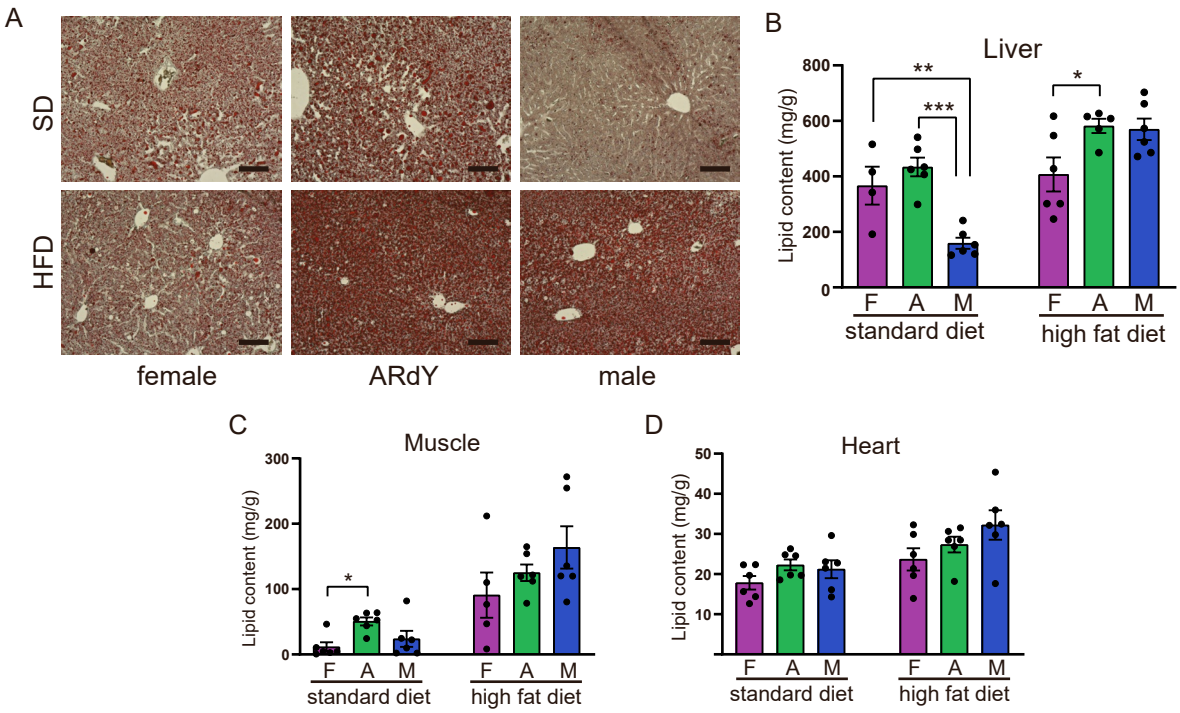

Supp. Fig. 3. Ectopic lipid deposition, related to Figure 3. (A) Oil Red O-stained liver sections from 15-week-old mice fed a standard diet or 8 weeks HFD. Scalebar = 100 um. (B) Lipid quantification in liver of 15-week-old mice fed a standard diet or 8 weeks HFD. (C) Lipid quantification in gastrocnemius muscle of 15-week-old mice fed a standard diet or 8 weeks HFD. (D) Lipid quantification in heart of 15-week-old mice fed a standard diet or 8 weeks HFD. Statistical significance in (B-D) was determined by ordinary one-way ANOVA with Tukey's multiple comparisons test. Abbreviations: F = female, A = ARdY, M = male, SD = standard diet, HFD = high fat diet.